

6-1-1989

# A Correction Algorithm for Particle-Size Distribution Measurements Made with the Forward-Scattering Spectrometer Probe

James A. Lock

Cleveland State University, j.lock@csuohio.edu

Edward A. Hovenac

Follow this and additional works at: [https://engagedscholarship.csuohio.edu/sciphysics\\_facpub](https://engagedscholarship.csuohio.edu/sciphysics_facpub)

 Part of the [Physics Commons](#)

**How does access to this work benefit you? Let us know!**

## *Publisher's Statement*

Copyright 1989 American Institute of Physics. This article may be downloaded for personal use only. Any other use requires prior permission of the author and the American Institute of Physics. The following article appeared in *Review of Scientific Instruments* 60 (1989): 1154-1160 and may be found at <http://link.aip.org/link/doi/10.1063/1.1140277>.

## Original Citation

Lock, James A. and Edward A. Hovenac. "A Correction Algorithm for Particle-Size Distribution Measurements Made with the Forward-Scattering Spectrometer Probe." *Review of Scientific Instruments* 60 (1989): 1154-1160.

## Repository Citation

Lock, James A. and Hovenac, Edward A., "A Correction Algorithm for Particle-Size Distribution Measurements Made with the Forward-Scattering Spectrometer Probe" (1989). *Physics Faculty Publications*. 60.

[https://engagedscholarship.csuohio.edu/sciphysics\\_facpub/60](https://engagedscholarship.csuohio.edu/sciphysics_facpub/60)

This Article is brought to you for free and open access by the Physics Department at EngagedScholarship@CSU. It has been accepted for inclusion in Physics Faculty Publications by an authorized administrator of EngagedScholarship@CSU. For more information, please contact [library.es@csuohio.edu](mailto:library.es@csuohio.edu).

# A correction algorithm for particle size distribution measurements made with the forward-scattering spectrometer probe

James A. Lock

*Physics Department, Cleveland State University, Cleveland, Ohio 44115*

Edward A. Hovenac

*Sverdrup Technology Inc., NASA Lewis Research Center, Cleveland, Ohio 44135*

(Received 17 November 1988; accepted for publication 8 February 1989)

Multiparticle coincidence events in the scattering volume of the forward-scattering spectrometer probe (FSSP) cause the instrument to bias the measurement of the particle size distribution of atmospheric aerosols toward large diameters. We employ a probabilistic model based on Poisson statistics to determine the average diameter and rms width of the actual size distribution as functions of the average diameter and rms width of the measured distribution. We compare our predictions to a Monte Carlo simulation of the FSSP operation

## INTRODUCTION

In an accompanying paper,<sup>1</sup> we examined a probabilistic model based on Poisson statistics for aerosol particles entering the scattering volume of the forward-scattering spectrometer probe (FSSP). We calculated the dead time and coincidence errors in the measured number density using this probabilistic model and compared them to the results of a Monte Carlo simulation of the FSSP operation. Given that the actual number density can be determined by this approach, we now employ our diagrammatic method of calculation to determine the connection between the measured particle size distribution and the actual size distribution. This is of interest because wind tunnel tests using the FSSP indicate that as the number density in the cloud increases, the FSSP skews the measured distribution toward larger diameters.<sup>2</sup> This effect is believed to be caused by multiparticle coincidences in the instrument's scattering volume.

As will be seen in the next section, the connection between the actual and measured size distributions is nonlinear, and as a result, standard deconvolution techniques are not applicable. As an alternative, we parametrize both the actual and measured distributions by their average diameters and root-mean-square (rms) widths. We then determine the actual average diameter and rms width as functions of the measured average diameter and width. In order to minimize the complexity of the calculations, we employ our probabilistic model in the limit of low number densities where only one- and two-particle coincidence events are important.

In any size distribution inversion scheme, the amount of information concerning the actual size distribution that can be recovered depends on one's state of knowledge of the measuring instrument. Complete instrument knowledge, in principle, allows complete distribution knowledge, and partial instrument knowledge allows only a knowledge of the gross characteristics of the size distribution. Recently, size distribution inversion schemes for an idealized particle counter and for the FSSP have been devised by Julanov, Lushnikov, and Nevskii<sup>3</sup> and by Cooper,<sup>4</sup> respectively. In both of these

articles, the authors are able to recover the actual size distribution because in Julanov and co-workers' idealized detector, the depth of the field region is identical to the entire scattering volume, and in Cooper's analysis of the FSSP, the signal and annulus gain functions are exactly known at all points in the scattering volume. Our approach is that if one only has knowledge of a few of the features of the signal and annulus gain factors, a partial particle size distribution inversion can still be accomplished and the average particle diameter and distribution width can be approximately recovered. In this way, this work represents a viewpoint complementary to that taken in Ref. 4.

In order to test a number of the assumptions that we make in deriving our inversion procedure, we compare our correction algorithm to the results of a Monte Carlo simulation of the FSSP operation. We find that under all circumstances examined, the correction algorithm represents a substantial improvement in the determination of the average diameter and rms width of the distribution over the uncorrected measured quantities.

## I. FSSP SCATTERING VOLUME GEOMETRY

As in Ref. 1, we consider a cylindrical optical scattering volume of diameter  $d$  and length  $L$  with uniform light intensity throughout the entire volume. For an individual FSSP instrument, the actual shape of the scattering volume may be more complicated than this idealized geometry. We employ this geometry for calculational simplicity, and its ultimate justification rests upon the comparison of our results with actual FSSP data. The near-forward-scattered light produced by a particle traversing the scattering volume at the location  $z$  along its axis is passed through a beam splitter and is focused on two photodiodes. The output voltages of the photodiodes are termed the signal voltage  $g_s(z)$  and the annulus voltage  $g_a(z)$ . Typical photodiode voltage profiles are shown in Fig. 1. The depth-of-field (DOF) region of the scattering volume is determined by a comparison of the two photodiode voltages and is defined to be the range of  $z$  locations for which

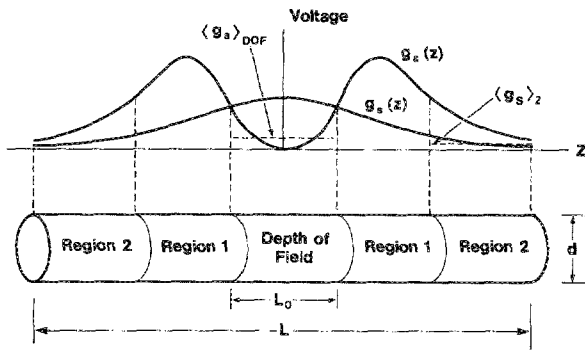


FIG. 1. The signal and annulus voltages as function of location in the optical scattering volume and the different regions of the scattering volume.

$$g_s(z) \geq g_a(z). \quad (1)$$

We take the length of the DOF to be  $L_0$  and let the average values of the signal and annulus voltages in the DOF region be given by

$$\langle g_s \rangle_{\text{DOF}} = \frac{1}{L_0} \int_{-L_0/2}^{L_0/2} g_s(z) dz, \quad (2)$$

and

$$\langle g_a \rangle_{\text{DOF}} = \frac{1}{L_0} \int_{-L_0/2}^{L_0/2} g_a(z) dz. \quad (3)$$

Events registered as being within the DOF are known as strobe events.

Baumgardner, Strapp, and Dye<sup>5</sup> further subdivide the portion of the scattering volume outside the DOF into two regions, denoted as regions 1 and 2. We do the same, but define the two regions slightly differently. Consider two particles of equal size passing through the scattering volume simultaneously, one of them being within the DOF and the other being outside the DOF at the location  $z$ . As is described in detail in Ref. 5, on the average a two-particle coincidence event is registered as occurring within the DOF if

$$\langle g_s \rangle_{\text{DOF}} + g_s(z) > \langle g_a \rangle_{\text{DOF}} + g_a(z), \quad (4)$$

and on the average it is registered as occurring outside the DOF if

$$\langle g_s \rangle_{\text{DOF}} + g_s(z) < \langle g_a \rangle_{\text{DOF}} + g_a(z). \quad (5)$$

We define the boundary between the two regions of the scattering volume outside the DOF as the location  $z$  where

$$g_a(z) = g_s(z) + \langle g_s \rangle_{\text{DOF}} - \langle g_a \rangle_{\text{DOF}}. \quad (6)$$

This is shown in Fig. 1. If the length of the scattering volume outside the DOF is

$$L_{12} = L - L_0, \quad (7)$$

then the length of region 1 in which Eq. (5) is valid is  $L_1$  and the length of region 2 in which Eq. (4) is valid is  $L_2$ . We also have

$$L_1 + L_2 = L_{12}. \quad (8)$$

For future use, we define the average value of the signal voltage in region 2 to be

$$\langle g_s \rangle_2 = \frac{1}{L_2} \left( \int_{-L/2}^{-L/2+L_2/2} g_s(z) dz + \int_{L/2-L_2/2}^{L/2} g_s(z) dz \right). \quad (9)$$

For most FSSP instruments,  $\langle g_s \rangle_2$  is of the order of 5%–10% of  $\langle g_s \rangle_{\text{DOF}}$ .

If the diameters of the aerosol particles are much larger than the wavelength of the laser light which produces the scattering volume, then the intensity of the near-forward-scattered light is approximately proportional<sup>6</sup> to the square of the particle diameter  $a$ . This proportionality is the origin of the four types of nonlinearities in the biasing of the size distribution. (1) Consider two identical particles of diameter  $a$  passing through the DOF simultaneously. These two are recorded as a single particle of diameter  $\sqrt{2}a$ . Thus, the size biasing is multiplicative rather than additive. (2) One cannot in general associate a given amount of multiplicative biasing with an  $m$ -particle coincidence event. Consider for example a three-particle coincidence event with all three particles passing through the DOF. This is recorded as a single particle of diameter  $\sqrt{3}a$  if all three of the particles are within the DOF at the same time. But it is recorded as a single particle of diameter  $\sqrt{2}a$  if the first particle leaves the DOF before the third particle enters it since the FSSP determines the effective particle size from the largest amplitude of the signal voltage in each event. (3) Consider a polydispersion of particle sizes. The biasing of the measured distribution mixes different particle sizes if two particles of different diameters are within the DOF at the same time. Thus, for a polydispersion, the total biasing is not the sum of the biasings of all the component particle sizes within the distribution. (4) Let the actual size distribution have  $N_1$  particles of diameter  $a_1$  and  $N_2$  particles of diameter  $a_2$ . Then if  $i$  and  $j$  are equal to 1 or 2, the probability of having a two-particle coincidence event with particles of diameters  $a_i$  and  $a_j$  is proportional to  $N_i N_j$ . As a result, when the measured size distribution is written in terms of the effective diameters of the particles recorded in multiparticle coincidence events, it takes the form of an expansion in terms of powers of the actual size distribution. This power-series expansion expresses the nonlinearity of the connection between the actual and measured distributions. There is another size biasing mechanism present in the FSSP as well. When large numbers of particles that are beyond the sensitivity range of the instrument pass through the scattering volume, they saturate the amplifier, cause baseline drift, and lengthen the instrument dead time. This can cause measured size distribution distortions. However, in the balance of this paper we assume that the instrument is set on a coarse enough scale so that this last type of distortion will not be a serious problem.

Let  $N(a)da$  be the number of particles in the actual size distribution with diameters between  $a$  and  $a + da$ . Similarly, let  $M(a)da$  be the number of events in the measured size distribution with effective diameters between  $a$  and  $a + da$ . An event is defined to begin when the first particle in a multiparticle coincidence enters the scattering volume and it ends when the last particle in the coincidence leaves the scattering

volume. Because of the size distribution biasing nonlinearities and our assumed incomplete knowledge of  $g_s(z)$  and  $g_a(z)$ , we will not attempt to explicitly connect  $M(a)$  and  $N(a)$ . Rather, we define the average diameter and the rms width of the actual distribution as

$$a_{\text{ave}}^{(a)} = \frac{1}{N} \int_0^\infty aN(a)da, \quad (10)$$

and

$$\sigma^{(a)} = \left( \frac{1}{N} \int_0^\infty (a - a_{\text{ave}}^{(a)})^2 N(a)da \right)^{1/2}, \quad (11)$$

respectively, where the total number of particles in the actual size distribution is

$$N = \int_0^\infty N(a)da. \quad (12)$$

Similarly, we define the average diameter and the rms width of the measured distribution as

$$a_{\text{ave}}^{(m)} = \frac{1}{M} \int_0^\infty aM(a)da, \quad (13)$$

and

$$\sigma^{(m)} = \left( \frac{1}{M} \int_0^\infty (a - a_{\text{ave}}^{(m)})^2 M(a)da \right)^{1/2}, \quad (14)$$

respectively, where the total number of events constituting the measured distribution is

$$M = \int_0^\infty M(a)da. \quad (15)$$

In the next section, we use a diagrammatic method of calculation to perform our size distribution inversion to determine  $a_{\text{ave}}^{(a)}$  and  $\sigma^{(a)}$  as functions of  $a_{\text{ave}}^{(m)}$  and  $\sigma^{(m)}$ .

Lastly, the particular strobe events which are used to determine the measured size distribution are termed valid counts. These are strobos which pass through the scattering volume near its widest point and spend an amount of time longer than the average transit time

$$\tau_{\text{ave}} = \int_0^\infty tQ(t)dt = \frac{\pi}{4} \frac{d}{v} \quad (16)$$

within the scattering volume, where  $v$  is the instrument air speed and

$$Q(t)dt = \begin{cases} \frac{t dt}{(d/v)[(d/v)^2 - t^2]^{1/2}}, & \text{for } t \leq d/v, \\ 0, & \text{for } t > d/v, \end{cases} \quad (17)$$

is the probability that a particle remains within the scattering volume for a time between  $t$  and  $t + dt$  once it has entered it for our idealized case of a cylindrical scattering volume.

## II. CALCULATION OF THE DISTRIBUTION AVERAGE SIZE AND RMS WIDTH

Consider the various types of coincidence scattering events. The probability  $P(m)$  that a scattering event is an  $m$ -particle coincidence event was calculated in Ref. 1, assuming that the arrival times of the particles participating in the event are described by Poisson statistics and taking into ac-

count the probability distribution  $Q(t)dt$ . Diagrams showing the output signal photodiode voltage as a function of time for one- and two-particle events in this model are given in Figs. 3(a)–3(c) of Ref. 1. In the limit of low number density, the leading term in the Taylor series expansion of  $P(m)$  was found to be

$$P(m) = \mathcal{O}(\beta^{m-1}), \quad (18)$$

where the expansion parameter is

$$\beta = (\pi/4)d^2L\mathcal{N}_a, \quad (19)$$

and  $\mathcal{N}_a$  is the actual number density of the aerosol. Let  $c_m$  be the probability that the duration of an  $m$ -particle event is longer than  $\tau_{\text{ave}}$ . For the one-particle event of Fig. 3(a) of Ref. 1, we find that

$$c_1 = \frac{1}{P(1)} \left( 1 - \int_{l=0}^{\tau_{\text{ave}}} Q(l)dl e^{-\lambda l} \right) \approx 0.62 + \mathcal{O}(\beta). \quad (20)$$

For the two-particle events of Figs. 3(b)–3(c) of Ref. 1, we find that

$$\begin{aligned} c_2 &= \frac{1}{P(2)} \left( 1 - \int_{l=0}^{\tau_{\text{ave}}} \int_{l'=0}^l \int_{l''=l-l'}^{\tau_{\text{ave}}-l''} Q(l)dl \right. \\ &\quad \times e^{-\lambda l} \lambda dt' Q(l')dl' e^{-\lambda l''} \\ &\quad \left. - \int_{l=0}^{\tau_{\text{ave}}} \int_{l'=0}^l \int_{l''=0}^{l-l'} Q(l)dl \right. \\ &\quad \left. \times e^{-\lambda l} \lambda dt' Q(l')dl' e^{-\lambda(l-l')} \right) \\ &\approx 0.97 + \mathcal{O}(\beta). \end{aligned} \quad (21)$$

At this point, a comment must be made about the FSSP measurement of valid counts. The instrument measures the transit time of each of the events occurring in the DOF. It computes the average transit time of all the strobos recorded thus far and compares the transit time of the next strobe to this average. If the particle number density is low, then most of the recorded strobos are one-particle events and the average transit time is well approximated by  $\tau_{\text{ave}}$ . If the number density is high, then the total number of strobos is dominated by multiparticle coincidence events. Since these events are of a longer duration, the average transit time will be much larger than  $\tau_{\text{ave}}$ . Thus, the calculation of the probabilities  $c_1$  and  $c_2$  in Eqs. (20) and (21) describes the selection of valid events in the low particle density regime only.

Putting together these various probabilities, the number of valid counts which are one-particle events and for which the diameter of the particle is between  $a$  and  $a + da$  is

$$n_e P(1) \frac{L_0}{L} c_1 \frac{N(a)da}{N}. \quad (22)$$

In this expression,  $n_e$  is the total number of events that occur anywhere within the scattering volume,  $P(1)$  is the fraction of them which are one-particle events,  $L_0/L$  is the fraction of them which occur within the DOF and are recorded as strobos,  $c_1$  is the fraction of them which are valid counts, and  $N(a)da/N$  is the fraction of them which have the proper diameter.

Two-particle events are recorded as strobos in one of

two ways, when both particles pass through the DOF and when one passes through the DOF and one passes through region 2 so that Eq. (4) is valid. Actually, this is true only if both particles have the same size. But we take Eq. (4) to be approximately true even if the two particles have different sizes. Following the same procedure as in relation (22), the number of valid counts which are two-particle events and for which the diameters of the two particles are between  $a$  and  $a + da$  and between  $a'$  and  $a' + da'$  is

$$n_e P(2) \frac{L_0^2}{L^2} c_2 \frac{N(a) da N(a') da'}{N^2} + n_e P(2) \frac{2L_0 L_2}{L^2} c_2 \frac{N(a) da N(a') da'}{N^2}. \quad (23)$$

For small number densities, Eq. (18) shows that coincidence events containing large numbers of particles have negligible probability. In this limit, we assume that only one- and two-particle events contribute to the total number of

Similarly,

$$a_{\text{ave}}^{(m)} = \frac{1}{M} \left( \int_0^\infty a n_e P(1) \frac{L_0}{L} c_1 \frac{N(a) da}{N} + \int_0^\infty \int_0^\infty (a^2 + a'^2)^{1/2} n_e P(2) \frac{L_0^2}{L^2} c_2 \frac{N(a) da N(a') da'}{N^2} + 2 \int_0^\infty \int_0^\infty (a^2 + \langle g_s \rangle_2 a'^2)^{1/2} n_e P(2) \frac{L_0 L_2}{L^2} c_2 \frac{N(a) da N(a') da'}{N^2} \right), \quad (27)$$

$$(a^2)_{\text{ave}}^{(m)} = \frac{1}{M} \left( \int_0^\infty a^2 n_e P(1) \frac{L_0}{L} c_1 \frac{N(a) da}{N} + \int_0^\infty \int_0^\infty (a^2 + a'^2) n_e P(2) \frac{L_0^2}{L^2} c_2 \frac{N(a) da N(a') da'}{N^2} + 2 \int_0^\infty \int_0^\infty (a^2 + \langle g_s \rangle_2 a'^2) n_e P(2) \frac{L_0 L_2}{L^2} c_2 \frac{N(a) da N(a') da'}{N^2} \right), \quad (28)$$

and

$$\sigma^{(m)} = [(a^2)_{\text{ave}}^{(m)} - (a_{\text{ave}}^{(m)})^2]^{1/2}. \quad (29)$$

Equations (27) and (28) require a number of comments. First, we assume that the output photodiode voltages are normalized so that

$$\langle g_s \rangle_{\text{DOF}} = 1.0. \quad (30)$$

As a result, the diameters of individual particles passing through the DOF appear in Eqs. (27) and (28) without being multiplied by gain factors. On the other hand, the signal voltage produced by a particle passing through region 2 of the scattering volume is proportional to  $\langle g_s \rangle_2 a^2$  on the average. This is because the light from such a particle is defocused at the photodiode position and is registered weaker than the light from a particle passing through the DOF which is focused on the photodiode position. Finally, the factor of 2 multiplying the last integral of Eqs. (27) and (28) takes into account the fact that the first particle may be within the DOF and the second particle is outside of it or the

valid counts. This is the same assumption that was made in Refs. 3 and 4. For this situation and neglecting terms of order  $\beta^2$  and higher, we obtain

$$P(1) \approx 1 - \beta, \quad (24)$$

$$P(2) \approx \beta, \quad (25)$$

and

$$M = \int_0^\infty n_e P(1) \frac{L_0}{L} c_1 \frac{N(a) da}{N} + \int_0^\infty \int_0^\infty n_e P(2) \frac{L_0}{L} \left( \frac{L_0}{L} + \frac{2L_2}{L} \right) c_2 \times \frac{N(a) da N(a') da'}{N^2} = n_e (1 - \beta) \frac{L_0}{L} c_1 + n_e \beta \frac{L_0}{L} \left( \frac{L_0 + 2L_2}{L} \right) c_2. \quad (26)$$

second particle may be within the DOF and the first particle is outside of it.

Equations (27) and (28) cannot be evaluated unless a particular form for  $N(a) da$  is assumed. In order to be able to perform all the integrals analytically, we assume that  $N(a) da$  contains particles of only three sizes, i.e.,

$$N(a) da = [B\delta(a - a_0 + \epsilon) + A\delta(a - a_0) + C\delta(a - a_0 - \epsilon)] da. \quad (31)$$

This distribution has the properties

$$N = A + B + C, \quad (32)$$

$$a_{\text{ave}}^{(a)} = a_0 + [(C - B)/N] \epsilon, \quad (33)$$

and

$$\sigma^{(a)} = [(C + B)/N]^{1/2} \epsilon. \quad (34)$$

Substituting Eq. (31) into Eqs. (27) and (28) and neglecting terms of order  $(\epsilon/a_0)^3$  and higher, we obtain

$$a_{\text{ave}}^{(m)} = \frac{1}{M} \left( n_e (1 - \beta) \frac{L_0}{L} c_1 a_{\text{ave}}^{(a)} + n_e \beta \frac{L_0^2}{L^2} c_2 (2)^{1/2} a_0 \left\{ 1 + \left( \frac{C - B}{N} \right) \frac{\epsilon}{a_0} + \left[ \frac{BC}{N^2} + \frac{A}{2N} \left( \frac{C + B}{2N} \right) \right] \frac{\epsilon^2}{a_0^2} \right\} + n_e \beta \frac{2L_0 L_2}{L^2} c_2 a_0 (1 + \langle g_s \rangle_2)^{1/2} \left\{ 1 + \left( \frac{C - B}{N} \right) \frac{\epsilon}{a_0} + \frac{4\langle g_s \rangle_2}{(1 + \langle g_s \rangle_2)^2} \left[ \frac{BC}{N^2} + \frac{A}{2N} \left( \frac{C + B}{2N} \right) \right] \frac{\epsilon^2}{a_0^2} \right\} \right), \quad (35)$$

and

$$(a^2)_{\text{ave}}^{(m)} = \frac{1}{M} \left\{ n_e (1 - \beta) \frac{L_0}{L} c_1 (a^2)_{\text{ave}}^{(a)} + n_e \beta \frac{L_0^2}{L^2} c_2 2a_0^2 \left[ 1 + 2 \left( \frac{C-B}{N} \right) \frac{\epsilon}{a_0} + \left( \frac{C+B}{N} \right) \frac{\epsilon^2}{a_0^2} \right] \right. \\ \left. + n_e \beta \frac{2L_0 L_2}{L^2} c_2 a_0^2 (1 + \langle g_s \rangle_2) \left[ 1 + 2 \left( \frac{C-B}{N} \right) \frac{\epsilon}{a_0} + \left( \frac{C+B}{N} \right) \frac{\epsilon^2}{a_0^2} \right] \right\}, \quad (36)$$

where

$$(a^2)_{\text{ave}}^{(a)} = \frac{1}{N} \int_0^\infty a^2 N(a) da \\ = a_0^2 + 2 \left( \frac{C-B}{N} \right) a_0 \epsilon + \left( \frac{C+B}{N} \right) \epsilon^2. \quad (37)$$

We next assume that the size distributions of interest are narrow enough and have a small enough skewness so that

$$\left( \frac{C-B}{N} \right) \left( \frac{\epsilon}{a_0} \right)^2 \approx 0. \quad (38)$$

Further we assume that  $\langle g_s \rangle_2$  is small enough so that

$$(\langle g_s \rangle_2)^2 \approx 0. \quad (39)$$

Then to first order in  $\beta$  Eqs. (26), (29), (35), and (36) become

$$a_{\text{ave}}^{(m)} = (1 + \beta K_1) a_{\text{ave}}^{(a)} + \beta K_2 (\sigma^{(a)})^2 / a_{\text{ave}}^{(a)}, \quad (40)$$

and

$$(\sigma^{(m)})^2 = \beta K_3 (a_{\text{ave}}^{(a)})^2 + (1 + \beta K_4) (\sigma^{(a)})^2, \quad (41)$$

where

$$K_1 = \frac{c_2}{c_1} \left( \frac{L_0}{L} (2^{1/2} - 1) + \frac{L_2}{L} \langle g_s \rangle_2 \right), \quad (42)$$

$$K_2 = \frac{c_2}{c_1} \left( \frac{L_0}{L} \frac{2^{1/2}}{4} + \frac{2L_2}{L} \langle g_s \rangle_2 \right), \quad (43)$$

$$K_3 = \frac{c_2}{c_1} \frac{L_0}{L} (3 - 2(2)^{1/2}), \quad (44)$$

and

$$K_4 = \frac{c_2}{c_1} \left[ \frac{L_0}{L} \left( \frac{2 - 2^{1/2}}{2} \right) - \frac{2L_2}{L} \langle g_s \rangle_2 \right]. \quad (45)$$

Finally, Eqs. (40) and (41) may be simultaneously solved to first order in  $\beta$  to give

$$a_{\text{ave}}^{(a)} = a_{\text{ave}}^{(m)} \left( \frac{1 + \beta K_4 - \beta K_2 (\sigma^{(m)})^2 / a_{\text{ave}}^{(m)2}}{1 + \beta (K_1 + K_4)} \right), \quad (46)$$

and

$$\sigma^{(a)} = \left( \frac{(\sigma^{(m)})^2 - \beta K_3 (a_{\text{ave}}^{(a)})^2}{1 + \beta K_4} \right)^{1/2}. \quad (47)$$

Equations (46) and (47) represent the connection between the average diameters and widths of the actual and measured size distributions. The connection does not require an exact knowledge of  $g_s(z)$  and  $g_a(z)$ , but only of their gross properties as parametrized by  $L$ ,  $L_0$ ,  $L_2$ , and  $\langle g_s \rangle_2$ . Many stringent assumptions were made in the derivation of these results. First, we assumed that the actual number density was small in order to consider only one- and two-particle coincidence events and to omit all terms of order  $\beta^2$  and

higher. In dense aerosols where the size distribution biasing is much greater, these terms of higher order in  $\beta$  describing coincidences of large numbers of particles are potentially very important. We can only hope that these higher-order terms, which we have not calculated, largely cancel each other for dense aerosols. Second, in order to be able to perform the integrals, we employed the unrealistic multi- $\delta$ -function size distribution. Again, we can only hope that our results are also valid for more realistic size distributions. Third, we assumed that the size distribution is not excessively wide or extremely skewed. Last, we assumed that the average signal voltage in region 2 is only a few percent of  $\langle g_s \rangle_{\text{DOF}}$ . In order to test this model and the idealizations upon which it is based, we compare the predictions of Eqs. (46) and (47) to the results of the Monte Carlo simulation of the FSSP operation described in Ref. 1.

### III. THE MONTE CARLO SIMULATION

In the Monte Carlo simulation of the FSSP operation, the scattering volume geometry was taken to be the idealized uniformly illuminated cylinder and the signal and annulus voltages for a particle of a given size were taken to be

$$g_s(z) = 1.3345(e^{-(z/0.004)^2} - 0.25e^{-(z/0.002024)^2}), \quad (48)$$

and

$$g_a(z) = 6.36(e^{-(z/0.004)^2} - 1.0e^{-(1/0.002024)^2}), \quad (49)$$

respectively for  $|z| \leq 0.008$ . For these voltages, according to Eq. (1) the DOF is the region  $|z| \leq 0.001$  and  $\langle g_a \rangle_{\text{DOF}}$  is calculated to be approximately

$$\langle g_a \rangle_{\text{DOF}} \approx 0.385. \quad (50)$$

In the DOF, the average value of the signal voltage is well approximated by Eq. (30). According to Eq. (6), the boundary between regions 1 and 2 of the scattering volume is  $z = 0.00579$ , giving

$$L_0/L = 0.125, \quad (51)$$

and

$$L_2/L = 0.316. \quad (52)$$

From Eq. (9) the average value of the signal voltage in region 2 is found to be approximately

$$\langle g_s \rangle_2 \approx 0.073, \quad (53)$$

which satisfies the approximation of Eq. (39). The diameter of the scattering volume was

$$d = 0.023 \text{ cm}, \quad (54)$$

and the light intensity within the scattering volume was as-

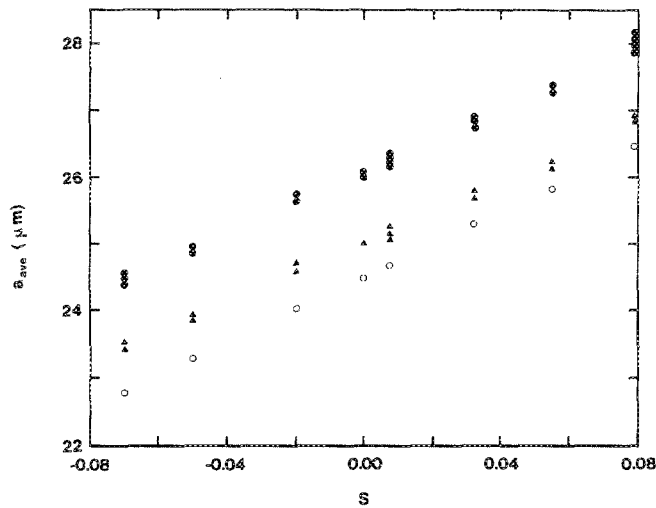


FIG. 2. The average diameter of the particle size distribution as a function of the distribution skewness. The open circles are the actual distribution average diameters, and the solid circles are the Monte Carlo simulation of the measured average diameters. The solid triangles are the reconstruction of the actual diameters from Eq. (46).

sumed to be uniform. The fast and slow reset times for the electronics were taken to be 2.3 and 6.0  $\mu\text{s}$ , respectively.

The Monte Carlo simulation input was either a Gaussian distribution of particle sizes with an adjustable average diameter and a rms width or a Weibull distribution of sizes with two adjustable parameters that were linear combinations of the average diameter, the rms width, and the skewness of the distribution.<sup>7</sup> The skewness of the distribution was defined as

$$S = (a_{\text{ave}} - a_{\text{max}})/a_{\text{max}}, \quad (55)$$

where  $a_{\text{max}}$  is the relative maximum of the  $N(a)da$  curve. A positive skewness corresponds to a tail at large particle sizes, and a negative skewness corresponds to a tail at small particle sizes.

The simulation was run for samples of 250 000 particles

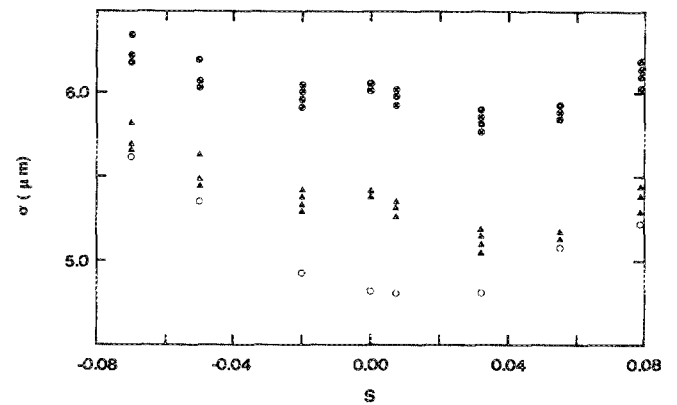


FIG. 3. The rms width of the particle size distribution as a function of the distribution skewness. The open circles are the actual distribution widths. The solid circles are the Monte Carlo simulation of the measured widths. The solid triangles are the reconstruction of the actual widths from Eq. (47).

entering the scattering volume. We obtained the following results. Figure 2 and 3 show the measured (i.e., Monte Carlo simulation output), actual (i.e., Monte Carlo simulation input), and our reconstructed [i.e., Eqs. (46) and (47)] average diameter and rms width as a function of actual distribution skewness for  $a_{\text{max}}^{(a)} = 24.5 \mu\text{m}$ ,  $\sigma^{(a)} \approx 5 \mu\text{m}$ , and for  $N_a = 500/\text{cm}^3$  corresponding to  $\beta = 0.3324$ . The data for the skewness  $S = 0$  was obtained from a Gaussian size distribution. For the range of skewnesses shown in Figs. 2 and 3, Eqs. (46) and (47) undercorrect the measured size distribution parameters with  $a_{\text{ave}}^{(m)}$  being about 106% of  $a_{\text{ave}}^{(a)}$  and our reconstruction of  $a_{\text{ave}}^{(a)}$  being about 102% of  $a_{\text{ave}}^{(a)}$ . Similarly, for the same range of skewnesses,  $\sigma^{(m)}$  is about 120% of  $\sigma^{(a)}$  and our reconstruction of  $\sigma^{(a)}$  is about 105% of  $\sigma^{(a)}$ . Similar data were also run for skewnesses as large as  $S \approx 0.22$  with the results that  $a_{\text{ave}}^{(m)}$  was about 112% of  $a_{\text{ave}}^{(a)}$  and Eq. (46) was about 107% of  $a_{\text{ave}}^{(a)}$ , with analogous results for the rms width. In Ref. 4 similar calculations were made for small

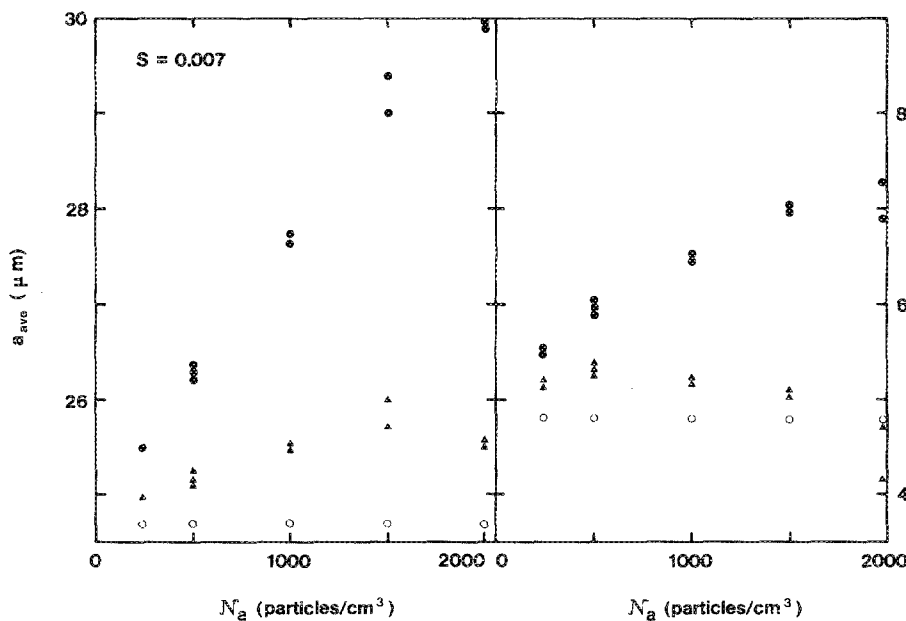


FIG. 4. The average diameter and rms width of the particle size distribution as a function of the actual number density for a distribution with skewness  $S = 0.007$ . The data points are as described in Figs. 2 and 3.

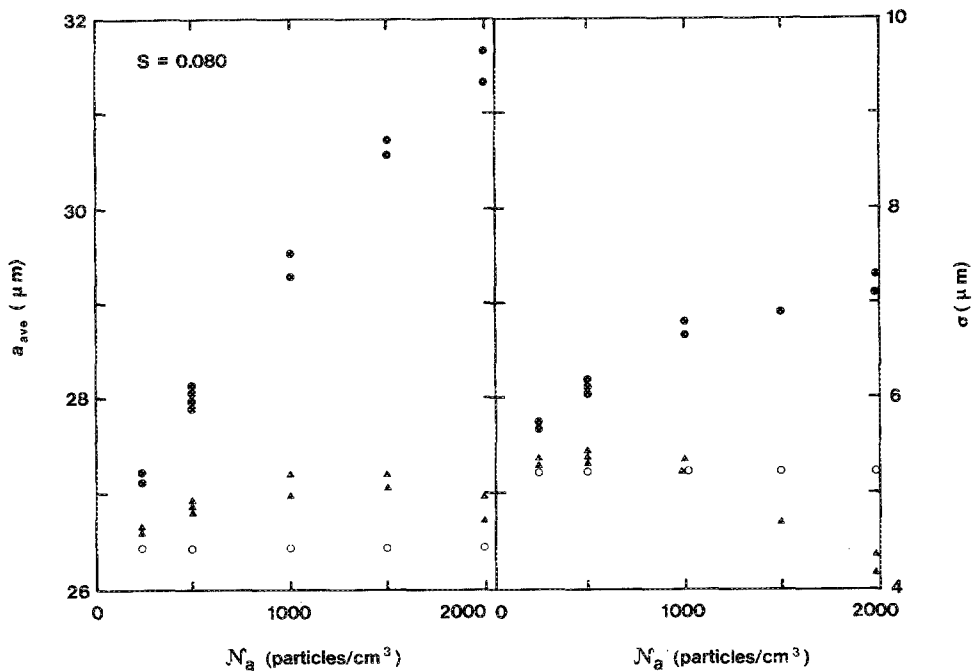


FIG. 5. The average diameter and rms width of the particle size distribution as a function of the actual number density for a distribution with skewness  $S = 0.080$ . The data points are as described in Figs. 2 and 3.

young cumulus clouds with an actual number density of  $500/\text{cm}^3$ . It was found that  $a_{\text{ave}}^{(m)}$  was 104.5% of  $a_{\text{ave}}^{(a)}$  and that  $\sigma^{(m)}$  was about 109% of  $\sigma^{(a)}$ . These results made with a different method of calculation are in reasonable agreement with our results of Figs. 2 and 3.

The Monte Carlo simulation was also run for particle number densities up to  $\mathcal{N}_a = 2000/\text{cm}^3$  for  $a_{\text{max}}^{(a)} = 24.5 \mu\text{m}$  and for  $S = 0.007$  and  $0.080$ . The results are shown in Figs. 4 and 5. For both skewnesses examined, the ratio  $a_{\text{ave}}^{(m)}/a_{\text{ave}}^{(a)}$  rapidly increases as  $\mathcal{N}_a$  increases. But the ratio of Eq. (46) over  $a_{\text{ave}}^{(a)}$  remains slightly higher than unity. The same may be said for the rms width of the size distribution. Again the results are in reasonable agreement with those of Ref. 4 where it was calculated that  $a_{\text{ave}}^{(m)}$  was 112.7% of  $a_{\text{ave}}^{(a)}$  for a monodispersion at a number density of  $1000/\text{cm}^3$ .

These results are both surprising and encouraging. Equations (46) and (47) were derived under very restrictive circumstances. But with realistic actual size distributions and with particle number densities large enough to have the situation dominated by many-particle coincidence events, these equations still reasonably well describe the size distribution biasing in the measurement process. As an added encouraging result, the numerical values of Eqs. (46) and (47) in Figs. 2–5 were found to be rather insensitive to the exact value of  $\langle g_s \rangle_2$ , with values between 0.06 and 0.12 giving roughly similar results. In Figs. 2–5 the difference between  $a_{\text{ave}}^{(m)}$  and  $a_{\text{ave}}^{(a)}$  is never more than about 30%. This is a reflection of the fact that the average particle diameter is a slowly varying function of changes in the shape of the size distribution. If the inversion results of Eq. (46) predicted a difference between actual and measured average diameters of sub-

stantially more than 30%, it would be a sign that one had a situation of very high number density and very high skewness, or a bimodal distribution. However, for these situations ideas such as average diameter and width distribution lose their utility anyway.

In summary, although the determination of exact relationship between the actual and measured size distributions is beset by many nonlinearities, the diagrammatic method of calculating probabilities that we employed in Ref. 1 appears to also adequately describe the biasing of reasonably well-behaved particle size distributions when they are parameterized by average diameters and rms widths.

#### ACKNOWLEDGMENT

One of us (J.A.L.) wishes to thank the Optical Systems Measurement Branch of the NASA Lewis Research Center for its hospitality and financial support during the summer 1988 when this work carried out under a NASA/ASEE Summer Faculty Fellowship.

- <sup>1</sup>J. A. Lock and E. A. Hovenac, *Rev. Sci. Instrum.* **60**, 1148 (1989).
- <sup>2</sup>E. A. Hovenac and R. F. Ide, AIAA paper No. 89-0769, Jan. 1989.
- <sup>3</sup>Yu. V. Julianov, A. A. Lushnikov, and I. A. Nevskii, *J. Aerosol Sci.* **15**, 69 (1984).
- <sup>4</sup>W. A. Cooper, *J. Atmos. Ocean. Technol.* **6** (to be published).
- <sup>5</sup>D. Baumgardner, W. Strapp, and J. E. Dye, *J. Atmos. Ocean. Technol.* **2**, 626 (1985).
- <sup>6</sup>H. C. van de Hulst, *Light Scattering by Small Particles* (Dover, New York, 1981), Secs. 9.31, 9.4, and 12.32.
- <sup>7</sup>K. C. Kapur and L. R. Lamberson, *Reliability in Engineering Design* (Wiley, New York, 1977), p. 292.